OPEN

Citation: Transl Psychiatry (2014) 4, e481; doi:10.1038/tp.2014.119

www.nature.com/tp

ORIGINAL ARTICLE

Time-dependent metabolomic profiling of Ketamine drug action reveals hippocampal pathway alterations and biomarker candidates

K Weckmann[1], C Labermaier[1], JM Asara[2], MB Müller[1,3] and CW Turck[1]

Ketamine, an *N*-methyl-*D*-aspartate receptor (NMDAR) antagonist, has fast-acting antidepressant activities and is used for major depressive disorder (MDD) patients who show treatment resistance towards drugs of the selective serotonin reuptake inhibitor (SSRI) type. In order to better understand Ketamine's mode of action, a prerequisite for improved drug development efforts, a detailed understanding of the molecular events elicited by the drug is mandatory. In the present study we have carried out a time-dependent hippocampal metabolite profiling analysis of mice treated with Ketamine. After a single injection of Ketamine, our metabolomics data indicate time-dependent metabolite level alterations starting already after 2 h reflecting the fast antidepressant effect of the drug. *In silico* pathway analyses revealed that several hippocampal pathways including glycolysis/gluconeogenesis, pentose phosphate pathway and citrate cycle are affected, apparent by changes not only in metabolite levels but also connected metabolite level ratios. The results show that a single injection of Ketamine has an impact on the major energy metabolism pathways. Furthermore, seven of the identified metabolites qualify as biomarkers for the Ketamine drug response.

Translational Psychiatry (2014) **4,** e481; doi:10.1038/tp.2014.119; published online 11 November 2014

INTRODUCTION

Psychiatric diseases including major depressive disorder (MDD) have a high morbidity and constitute an ever increasing burden for societies.[1] At present, most clinically used antidepressants are targeting monoaminergic reuptake mechanisms.[2] However, a limited efficacy and a delayed onset of therapeutic response combined with several side effects make them less than ideal drugs. Approximately one-third of patients are suffering from treatment-resistant depression and do not respond to commonly used antidepressants.[3] Reasons for the delayed therapeutic effect and treatment-resistant depression remain mysterious. To improve antidepressant drug efficacy, one line of research has focused on the *N*-methyl-*D*-aspartate receptor (NMDAR) and its signaling pathways, with the goal to manipulate glutamatergic neurotransmission, which has been associated with MDD pathobiology. Ketamine targets the glutamatergic system by blocking the NMDAR with profound effects on downstream signaling cascades.[4–7] Unlike selective serotonin reuptake inhibitor (SSRI) medications that result in a delayed onset of therapeutic response, Ketamine improves depressive symptoms within hours and is particularly effective in patients suffering from treatment-resistant depression.[8–16]

Studies on Ketamine's mode of action in rodents have shown antidepressant-like effects in several behavioral tests including Learned Helplessness, Forced Swim Test (FST), Chronic Mild Stress and Novelty Suppressed Feeding Test.[17–22] On the molecular level, Ketamine activates the mammalian target of rapamycin signaling pathway, α-amino-3-hydroxy-5-methyl-4-isoxazolepropionic receptors and brain-derived neurotrophic factor synthesis, ultimately resulting in an elevated number of dendritic spines.[23]

Psychomimetic side effects have so far prevented Ketamine's routine use in the clinic as a first-line drug. In order to develop alternative fast-acting drugs with a similar mode of action on the glutamatergic system, but with fewer side effects, a detailed understanding of the molecular events elicited by Ketamine treatment is essential.

The hippocampus was chosen as a relevant brain region for studying MDD molecular pathways.[24–28] Decreased hippocampal volumes during acute depressive episodes, observed with magnetic resonance imaging analyses, are believed to be involved in the pathobiology of MDD.[29–32] These changes are present during an acute episode of MDD and are already apparent during the first depressive episode.[33] Possible causes of the hippocampal volume reduction include neuronal cell loss,[34] pruning of apical dendrites in the CA3 subregion, decreased dentate gyrus neurogenesis[35] and a loss of glial cells.[36] Antidepressant treatment can reverse these effects and hippocampal volume decrease seems to be less prominent or even absent in phases of remission.[30] Patients suffering from MDD show impairments in their memory, which is highly dependent on the hippocampus,[37] and there is a dysregulated connectivity network of several brain regions in MDD including the hippocampus.[38]

Alterations affecting the metabolome are a reflection of modified pathway activities in response to drug treatment.[39,40] In the present study, C57BL/6 mice were treated with a single injection of Ketamine with the aim of identifying hippocampal

[1]Department of Translational Research in Psychiatry, Max Planck Institute of Psychiatry, Munich, Germany and [2]Division of Signal Transduction, Department of Medicine, Beth Israel Deaconess Medical Center, Harvard Medical School, Boston, MA, USA. Correspondence: Professor CW Turck, Department of Translational Research in Psychiatry, Max Planck Institute of Psychiatry, Kraepelinstrasse 2–10, Munich 80804, Germany.
E-mail: turck@mpipsykl.mpg.de
[3]Present address: Division of Experimental Psychiatry, Department of Psychiatry and Psychotherapy and Focus Program Translational Neuroscience (FTN), Johannes Gutenberg University Medical Center, Untere Zahlbacher Strasse 8, Mainz 55131, Germany.
Received 1 July 2014; revised 12 September 2014; accepted 28 September 2014

cellular pathway alterations and biomarker candidates with the help of a sensitive metabolomics platform.[41]

MATERIALS AND METHODS

Animals and Ketamine treatment

Eight-week-old male C57BL/6 mice (Charles River Laboratories, Maastricht, the Netherlands) were first singly housed for 2 weeks under standard conditions (12-h light/dark cycle, lights on at 0600 hours, room temperature 23 ± 2 °C, humidity 60%, tap water and food *ad libitum*) in the facilities of the Max Planck Institute of Psychiatry. After habituation, the mice were treated intraperitoneally with S-Ketamine (3 mg kg^{-1}, Pfizer, Karlsruhe, Germany) or vehicle (0.9% saline solution). Two, fourteen, twenty-four and seventy-two hours after Ketamine treatment, an FST was performed measuring the antidepressant-like behavior and afterwards animals were killed by an overdose of isoflurane (Forene, Abbott, Wiesbaden, Germany). The animals were perfused with 0.9% ice-cold saline solution. Mice were decapitated and their brains were harvested and dissected. Total hippocampi were shock-frozen in liquid nitrogen and stored at − 80 °C until further analysis. The experiments were performed in accordance with the European Communities Council Directive 86/609/EEC. The protocols were approved by the committee for the Care and Use of Laboratory Animals of the Government of Upper Bavaria, Germany.

Forced Swim Test

Each mouse was put into a 2-l glass beaker (diameter: 13 cm, height: 24 cm) filled with tap water (21 ± 1 °C) to a height of 15 cm, so that the mouse could not touch the bottom with its hind paws or tail. Testing duration was 6 min and at the end of the test the animals were immediately dried with a towel and returned to their home cage. The immobility time was scored 2 h (Ketamine-treated animals: $n = 33$, vehicle-treated animals: $n = 33$), 14 h (Ketamine-treated animals: $n = 31$, vehicle-treated animals: $n = 29$), 24 h (Ketamine-treated animals: $n = 33$, vehicle-treated animals: $n = 33$) and 72 h (Ketamine-treated animals: $n = 31$, vehicle-treated animals: $n = 29$) after Ketamine treatment by an experienced observer, blind to the condition of the animals.

Isolation of membrane-associated proteins

Membrane-associated proteins were prepared by repeated tissue homogenization and extraction of nonmembrane proteins and solubilization with sodium dodecyl sulfate (SDS). Hippocampi were homogenized for 30 s in 1 ml of 2 M NaCl, 10 mM HEPES/NaOH, pH 7.4, 1 mM EDTA containing protease inhibitor cocktail Tablets 'cOmplete' (Roche Diagnostics, Mannheim, Germany), then incubated for 10 min and homogenized again for 30 s and further with a ultrasonicator for 3 × 10 s on ice. The homogenates were centrifuged at 16 100 *g* at 4 °C for 20 min. The pellets were rehomogenized in 1 ml of 0.1 M Na_2CO_3 and 1 mM EDTA, pH 11.3, mixed at 4 °C for 30 min and collected by centrifugation (16 100 *g* at 4 °C for 20 min). Subsequently, the pellets were extracted with 5 M urea, 100 mM NaCl, 10 mM HEPES, pH 7.4 and 1 mM EDTA and then washed twice with 0.1 M Tris/HCl, pH 7.6. The pellets were solubilized in 50 µl of 2% SDS, 50 mM dithiothreitol and 0.1 M Tris/HCl, pH 7.6, at 90 °C for 1 min and stored at − 20 °C until further analysis.

Western blotting

Hippocampal membrane-associated proteins from 8-week-old male C57BL/6 mice treated with Ketamine for 2 h (Ketamine-treated animals: $n = 4$, vehicle-treated animals: $n = 5$), 14 h (Ketamine-treated animals: $n = 5$, vehicle-treated animals: $n = 4$), 24 h (Ketamine-treated animals: $n = 5$, vehicle-treated animals: $n = 5$) and 72 h (Ketamine-treated animals: $n = 5$, vehicle-treated animals: $n = 3$) were fractionated by SDS-polyacrylamide gel electrophoresis with 12% separating gels and western blotting was performed based on standard protocols. After electrophoresis, proteins were transferred to polyvinylidene difluoride membranes (Immobilon-P, Millipore, Billerica, MA, USA). The primary antibody was against the subunit A of the succinate dehydrogenase complex (Anti-SDHA, 1:200, sc98253, Santa Cruz Biotechnology, Dallas, TX, USA). An anti-rabbit ECL horseradish peroxidase-linked secondary antibody (1:10 000; NA934, GE Healthcare Life Sciences, Little Chalfont, Buckinghamshire, UK) was used. The densitometric analyses were performed with the Image Lab software (Bio-Rad Laboratories, Munich, Germany).

Targeted metabolomics analysis

Five hippocampal tissues per treatment and time point were homogenized (2 min × 1200 min^{-1}, homogenizer PotterS, Sartorius, Göttingen, Germany) in 30-fold ice-cold 80% methanol. Samples were centrifuged (14 000 *g*, 10 min, 4 °C) and the supernatants were incubated on dry ice. Afterwards, the pellets were incubated in sixfold ice-cold 80% methanol and then combined with the previous supernatants. The metabolite extracts were vortexed, centrifuged (14 000 *g*, 10 min, 4 °C), lyophilized and then stored at − 80 °C until further analysis. Samples were resuspended using 20 µl liquid chromatography-mass spectrometry grade water. Ten microliters were injected and analyzed using a 5500 QTRAP triple quadrupole mass spectrometer (AB/SCIEX, Framingham, MA, USA) coupled to a Prominence UFLC high-performance liquid chromatography system (Shimadzu, Columbia, MD, USA) via selected reaction monitoring of a total of 254 endogenous water-soluble metabolites for steady-state analyses of samples. Samples were delivered to the mass spectrometer via normal phase chromatography using a 4.6-mm i.d × 10 cm Amide Xbridge HILIC column (Waters, Milford, MA, USA) at 350 µl min^{-1}. Gradients were run starting from 85% buffer B (high-performance liquid chromatography grade acetonitrile) to 42% B from 0 to 5 min; 42% B to 0% B from 5 to 16 min; 0% B was held from 16 to 24 min; 0% B to 85% B from 24 to 25 min; 85% B was held for 7 min to re-equilibrate the column. Buffer A comprised 20 mM ammonium hydroxide/20 mM ammonium acetate (pH = 9.0) in 95:5 water:acetonitrile. Some metabolites were targeted in both positive and negative ion modes for a total of 285 selected reaction monitoring transitions using positive/negative polarity switching. Electrospray ionization voltage was +4900 V in positive ion mode and − 4500 V in negative ion mode. The dwell time was 4 ms per selected reaction monitoring transition and the total cycle time was 1.89 s. Approximately 9–12 data points were acquired per detected metabolite. Peak areas from the total ion current for each metabolite-selected reaction monitoring transition were integrated using the MultiQuant v2.0 software (AB/SCIEX). Animals from the same cohort were used for all metabolomic analyses.

Statistics and data analyses

Identification of significant metabolite alterations. Metabolite intensities were median-normalized and auto-scaled for statistical analysis. Significant metabolite level changes 2, 14, 24 and 72 h upon Ketamine treatment were identified by multivariate Partial Least Squares—Discriminant Analyses (PLS-DA) and high-dimensional feature selection significance analysis of microarrays (and metabolites; SAM) using MetaboAnalyst (http://www.metaboanalyst.ca).[42–44] The quality of the PLS-DA models was assessed for R^2, Q2 and accuracy with variable influence of projection (VIP) score $\geqslant 1.0$ and for SAM with $q \leqslant 0.1$ and false discovery rate $\leqslant 0.1$. We improved robustness of our data analyses and increased confidence in significantly altered metabolites and enriched pathways by only considering the overlap between the two different statistical methods.

Identification of significantly enriched pathways. Pathway analyses were performed for each time point using MetaboAnalyst (http://www.metaboanalyst.ca) applying a hypergeometric algorithm for over-representation analysis and relative-betweeness centrality for pathway topology analysis.[43,45,46] Pathways were considered affected if they were significantly enriched ($P_{\text{Holm-corrected}} \leqslant 0.1$) for all significantly altered metabolites of an individual time point.

Calculation of metabolite pair ratios. The median-normalized metabolite intensities before auto-scaling of selected pairs of metabolites were used to calculate metabolite ratios. For statistical analyses, Student's *t*-test was performed by using the metabolite ratio of interest for each Ketamine- and vehicle-treated animal (for example, metabolite x/metabolite y of one Ketamine-treated animal) calculated by dividing the metabolite intensity of metabolite x by the intensity of metabolite y for each time point. The final metabolite ratio of interest (for example, metabolite x/metabolite y for all Ketamine- and vehicle-treated animals) was then calculated by dividing the average metabolite intensities of all Ketamine-treated animals by the average metabolite intensities of all vehicle-treated animals.

Identification of metabolite biomarker candidates. Antidepressant treatment hippocampal metabolite biomarker candidates were detected by applying multivariate PLS-DA models taking the VIP scores (VIP score $\geqslant 1.0$) and SAM with $q \leqslant 0.1$ and false discovery rate $\leqslant 0.1$ into account. The quality of the PLS-DA models was assessed in terms of R^2, Q2 and accuracy. Metabolites qualified as biomarker candidates if they had a consistent VIP

score $\geqslant 1.0$ for the 2-, 14- and 24-h time points for which good and robust PLS-DA models had been determined. In addition, they required $q \leqslant 0.1$ for at least one of the time points.

RESULTS

C57BL/6 wild-type mice were assessed at different time points with regard to antidepressant-like behavior using the FST after receiving a single injection of Ketamine ($3\,mg\,kg^{-1}$; Supplementary Figure 1). In order to avoid any behavioral habituation, independent groups of mice were examined for their FST immobility time. A two-way analysis of variance showed no statistically significant interaction between the effects of treatment and different time points on the FST immobility time. The main effects analysis showed a significant reduction in FST immobility time when comparing Ketamine with vehicle-treated animals and significant alterations for the different time points. Therefore, no treatment effects for the individual time points were examined. A Tukey's honest significant difference test revealed a statistically significant difference in FST immobility time between the 2h (Ketamine-treated animals: $n = 33$, vehicle-treated animals: $n = 33$), 14 h (Ketamine-treated animals: $n = 31$, vehicle-treated animals: $n = 29$) and 72 h (Ketamine-treated animals: $n = 31$, vehicle-treated animals: $n = 29$) time points, between the 14- and 24-h (Ketamine-treated animals: $n = 33$, vehicle-treated animals: $n = 33$) time points and between the 24- and 72-h time points. On the basis of these results, we chose five mice per time point and group for the metabolomic analyses.

After a single injection of Ketamine, a total of 226, 218, 227 and 221 metabolites were quantified in the hippocampus for the 2-, 14-, 24- and 72-h time points, respectively (Supplementary Table 1).

The metabolite profiles separated Ketamine from vehicle-treated mice using multivariate PLS-DA for all time points (Figure 1). The quality criteria (Supplementary Figure 2A) of PLS-DA models were assessed for R^2, Q2 and accuracy values. They indicate good and robust models, with the exception of the 72-h time point. The weak PLS-DA model of the 72-h time point can result in false-positives. Nevertheless, the results were included as they are another indication of Ketamine's fast antidepressant-like effect on the metabolome.

For the identification of metabolite changes characteristic for group separation, the VIP parameter was used. The VIP indicates the importance of each metabolite for group separation. Only metabolites with VIP values $\geqslant 1.0$ were selected and used for further data analysis. To increase the robustness of our analyses, we additionally combined the PLS-DA with a high-dimensional feature selection, SAM analysis, to obtain a complete list of metabolites for each time point that significantly contribute to Ketamine drug action (Supplementary Table 2). Two hours after a single injection of Ketamine 45 metabolite levels were significantly altered (Supplementary Table 2A), with 21 metabolites reduced and 24 metabolites upregulated in Ketamine compared with vehicle-treated mice (Supplementary Table 2A). For the 14- and 24-h time points, 22 and 11 metabolites, respectively, were detected at lower levels (Supplementary Tables 2B and 2C). In agreement with the observation that the PLS-DA model of the 72-h time point is not robust, no significant metabolite alterations were found 72 h after Ketamine treatment.

Next, we interrogated the significantly altered metabolites to delineate affected hippocampal pathways (Table 1). Citrate cycle, glycine, serine and threonine metabolism and pyrimidine metabolism were significantly enriched 2 h after a single injection of Ketamine. Pentose phosphate and glycolysis/gluconeogenesis pathways were significantly enriched for the 14-h time point (Table 1).

Interestingly, based on KEGG database information all five pathways are interconnected by shared metabolites (Supplementary Figure 3). Several previous analyses by us and others have also shown an involvement of the citrate cycle in psychiatric phenotypes.[47–49] The citrate cycle consists of a series of biochemical reactions to generate high levels of energy through the connected oxidative phosphorylation (OXPHOS) pathway. In our analysis we show for the first time that Ketamine has an impact on the citrate cycle by altering several of its metabolite levels. Already 2 h after a single injection of Ketamine, thiamine pyrophosphate (2 h: FC = 1.43 (data not shown)), acetyl-CoA (2 h: FC = 1.49) and succinate (2 h: FC = 1.96) levels were significantly increased. Succinate-CoA (2 h: FC = 1.44) showed a high, but not significant, FC 2 h after Ketamine treatment. Fumarate (2 h: FC = 0.79) levels were significantly reduced 2 h after Ketamine injection and malate levels (2 h: FC = 0.82, 14 h: FC = 0.82) were significantly decreased for the 2- and 14-h time points. Isocitrate (2 h: FC = 0.64) tended to be downregulated and citrate (2 h: FC = 0.68) levels were lower, albeit with not a significant FC 2 h after a single injection of Ketamine. Oxaloacetate (2 h: FC = 1.17) and alpha-ketoglutarate (2 h: FC = 0.99) levels were unchanged (Figure 2a and Supplementary Table 2). Selected pairs of metabolite concentrations (metabolite ratios) can indicate alterations in enzyme activity or expression rate.[50] Metabolite ratios of the citrate cycle were calculated (Figure 2a and Supplementary Figure 4). The ratios are indicated by boxes, whereby each box represents a time point (from left to right 2, 14, 24 and 72 h). Significant metabolite ratio differences or trends are illustrated in pink (increased ratio) and black (decreased ratio). The citrate/acetyl-CoA ratio (2 h: ratio = 0.46) is significantly decreased 2 h after Ketamine treatment. Alpha-ketoglutarate/isocitrate metabolite ratios (2 h: ratio = 1.56, 24 h: ratio = 1.63) tended to be increased for the 2- and 24-h time points and the fumarate/succinate ratio (2 h: ratio = 0.40, 14 h: ratio = 0.55) tended to be lower at 2 h and was significantly decreased at 14 h after a single injection of Ketamine (Figure 2a and Supplementary Figure 4). Subunit A of the SDHA complex catalyzes the succinate to fumarate reaction as part of the citrate cycle. We therefore investigated whether this could be caused by altered SDHA protein levels following drug treatment. Indeed, we found such a difference when comparing hippocampal protein extracts from Ketamine- and vehicle-treated mice. Western blot analyses indicated that at the 2-h (Ketamine-treated animals: $n = 4$, vehicle-treated animals: $n = 5$; FC = 1.81) and 24-h (Ketamine-treated animals: $n = 5$, vehicle-treated animals: $n = 5$; FC = 1.99) time points a significant upregulation of SDHA protein can be observed upon Ketamine treatment (Figure 2b).

As the citrate cycle produces energy equivalents in form of GTP and NADH as well as ultimately ATP through complex V of the OXPHOS pathway, we analyzed the GTP, NADH and ATP levels upon Ketamine treatment (Figure 2c and e). GTP levels were significantly increased at the 2-h and downregulated at the 24-h time points (Figure 2c). Metabolite levels tended to be upregulated at 14 h for NADH (Figure 2d). ATP levels tended to be increased 14 h in Ketamine- compared with vehicle-treated mice and were significantly decreased at the 24-h time point (Figure 2e).

The glycolysis/gluconeogenesis pathway was also enriched upon Ketamine treatment. Almost all quantified metabolites were significantly altered 14 h after a single injection of Ketamine (Figure 3a). Glucose-6-phosphate (14 h: FC = 0.53), fructose-6-phosphate (14 h: FC = 0.40), fructose-1,6-bisphosphate (14 h: FC = 0.58) and dihydroxy-acetone-phosphate (14 h: FC = 0.24) were significantly downregulated. In contrast, 3-phosphoglycerate (2 h: FC = 1.75, 14 h: FC = 2.02) was significantly upregulated at the 2- and 14-h time points; phosphoenolpyruvate (2 h: FC = 1.75) levels were found to be significantly upregulated 2 h after Ketamine treatment and pyruvate was unchanged. Furthermore, comparing the FCs, q-values and VIP scores of all metabolites of the glycolysis pathway, we were able to show that with the exception of 3-

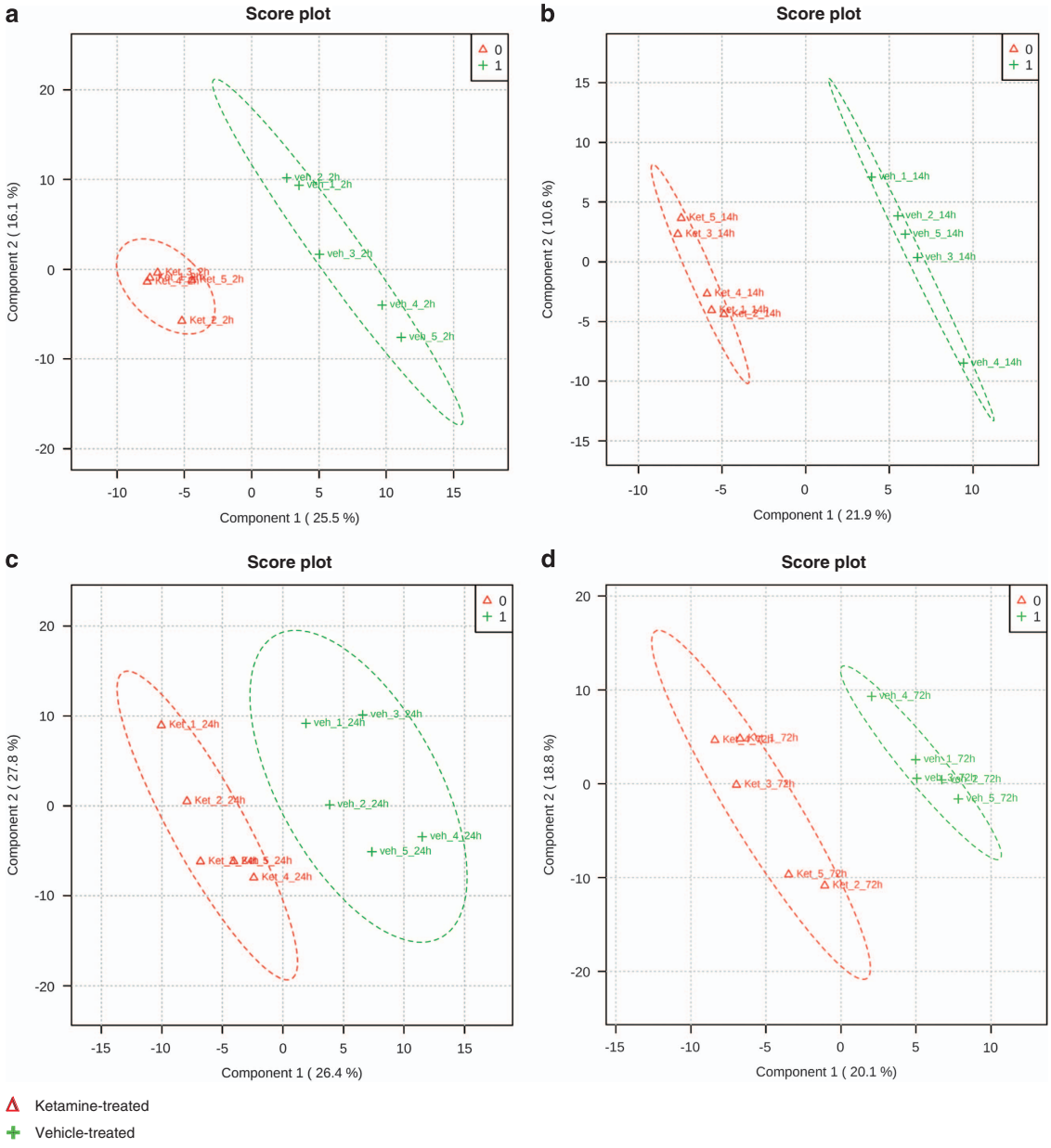

Figure 1. Multivariate partial least squares-discriminant analysis (PLS-DA) of (**a**) 2-h, (**b**) 14-h, (**c**) 24-h and (**d**) 72-h time course comparison after a single injection of Ketamine (3 mg kg^{-1}) or vehicle using all quantified metabolites for each time point. All R^2, Q2 and accuracy values indicate good (2 h: $R^2 = 0.99$, $Q^2 = 0.60$, accuracy = 1.0; 14 h: $R^2 = 1.0$, $Q^2 = 0.63$, accuracy = 1.0) and robust (24 h: $R^2 = 0.92$, $Q^2 = 0.52$, accuracy = 0.8) models with the exception of the 72-h time point ($R^2 = 1.0$, $Q^2 = 0.29$, accuracy = 0.6). $N = 5$ mice per group and time point. See also Supplementary Figure 2.

phosphoglycerate and phosphoenolpyruvate, all metabolites showed the same pattern (Figure 3b). We also calculated the metabolite ratios for the glycolytic pathway (Figure 3a and Supplementary Figure 4). The fructose-6-phosphate/glucose-6-phosphate ratio (14 h: ratio = 1.64) tended to be elevated 14 h after Ketamine treatment. The fructose-1,6-phosphate/fructose-6-phosphate metabolite ratio (72 h: ratio = 0.48) showed a significant decrease at the 72-h time point. However, as the PLS-DA resulted in a weak model for this time point, the decreased fructose-1,6-phosphate/fructose-6-phosphate metabolite ratio might be a false-positive. The glyceraldehyde-3-phosphate/dihydroxy-acetone-phosphate ratio (14 h: ratio = 0.84) was significantly lower and the 3-phosphoglycerate/glyceraldehyde-3-phosphate ratio (14 h: ratio = 4.51, 24 h: ratio = 2.37) was significantly increased 14 h after a single injection of Ketamine and tended to be upregulated for the 24-h time point. The 3-phosphoglycerate/phosphoenolpyruvate (14 h: ratio = 0.47) and pyruvate/phosphoenolpyruvate ratios (2 h: ratio = 0.61) were either significantly or tended to be lower, respectively (Figure 3a and Supplementary Figure 4).

We next attempted to identify metabolite biomarkers for the Ketamine treatment response. PLS-DA models can be used for biomarker discovery taking the VIP scores into account. When PLS-DA for the 2-, 14-, 24- and 72-h time points were assessed for quality criteria (Supplementary Figure 2 A), all R^2, Q2 and accuracy values indicate good and robust models, with the exception of the 72-h time point. On the basis of these results, we chose metabolites that are important and stable contributors for group separation with a consistent VIP score $\geqslant 1.0$ for the 2-, 14- and 24-h time points and with $q \leqslant 0.1$ for at least one of the time points.

Table 1. Pathway analyses of significantly altered metabolites (PLS-DA VIP ⩾ 1.0, SAM, FDR ⩽ 0.10, SAM $q \leqslant 0.1$) 2 and 14 h after a single injection of Ketamine (3 mg kg^{-1})

Pathway	P-*value*	$P_{\text{Holm-corrected}}$ *value*	*FDR*	*Metabolite*	*Time point (h)*
Citrate cycle	0.000012	0.00095	0.0006	Fumarate	2
				Succinate	2
				Thiamine pyrophosphate	2
				Phosphoenolpyruvate	2
				Acetyl-CoA	2
				Malate	2 /14
Glycine, serine and threonine metabolism	0.000016	0.00127	0.0006	Glyoxylate	2
				Betaine aldehyde	2
				Betaine	2
				Choline	2
				Glycerate	2
				Serine	2
				Cystathionine	2
				3-Phosphoglycerate	2
Pyrimidine metabolism	0.000855	0.06841	0.0234	Ureidosuccinate	2
				Cytidine	2
				Thymidine	2
				Uridine	2
				Uridine 5'-monophosphate (UMP)	2
				Cytidine diphosphate (CDP)	2
				Methylmalonate	2
Pentose phosphate pathway	0.000004	0.00036	0.0004	Glucose-6-phosphate	14
				6-Phospho-D-gluconate	14
				Fructose-6-phosphate	14
				Fructose-1,6-bisphosphate	14
				Erythrose-4-phosphate	14
Glycolysis/gluconeogenesis	0.000432	0.03501	0.0177	Fructose-6-phosphate	14
				Fructose-1,6-bisphosphate	14
				Glucose-6-phosphate	14
				Dihydroxy-acetone-phosphate	14
				Glyceraldehdye-3-phosphate	14

Abbreviations: FDR, false discovery rate; PLS-DA, partial least square-discriminant analysis; SAM, significance analysis of microarrays (and metabolites); VIP, variable importance in projection. $N = 5$ mice per group and time point.

This resulted in seven metabolite biomarker candidates for Ketamine drug action (Supplementary Figure 2B).

DISCUSSION

Metabolomics provides an analytical tool for the identification of pathway alterations and drug targets.[39,51–54] To our knowledge, this is the first study that identifies metabolite alterations, affected pathways and biomarker candidates for the Ketamine treatment response in mice.

Our results indicate significant metabolite level and metabolite ratio changes that are part of several pathways including citrate cycle, glycine, serine and threonine metabolism, pyrimidine metabolism, pentose phosphate pathway and glycolysis/gluconeogenesis (Table 1). Mitochondrial abnormalities including alterations in energy metabolism such as citrate cycle and glycolysis have previously been implicated in the pathobiology of affective disorders.[47–49,55–60] We observed several metabolite level and metabolite ratio changes of the citrate cycle already 2 h after Ketamine treatment (fumarate, malate, citrate and isocitrate, alpha-ketoglutarate/isocitrate levels increase; succinate, acetyl-CoA and succinate-CoA, citrate/acetyl-CoA and succinate/fumarate levels decrease; Figure 2a). Alterations in metabolite ratios can reflect changes in enzyme activities or protein expression. Interestingly, pyruvate dehydrogenase, isocitrate dehydrogenase and SDH are part of or connected to the citrate cycle and regulated by Ca^{2+}.[61] Ketamine blocks the NMDAR resulting in a decreased Ca^{2+} flux into the cell and mitochondria, which ultimately could be the cause for an inactivation of these enzymes and the here observed metabolite level and metabolite ratio alterations. Decreased isocitrate/alpha-ketoglutarate and succinate/fumarate ratios as well as altered SDHA protein levels further support this hypothesis.

The energy equivalents GTP and NADH are produced through the citrate cycle and ATP via the connected OXPHOS pathway. GTP is generated during the transformation of succinate-CoA to succinate. We observed significantly higher levels of succinate after Ketamine treatment possibly resulting in elevated GTP levels. We could show a significant upregulation of GTP (Figure 2c) already 2 h upon Ketamine treatment; 14 h after a single injection of Ketamine, NADH and ATP levels tended to be increased (Figure 2d and e). GTP and ATP levels were significantly reduced for the 24-h time point when comparing Ketamine- with vehicle-treated mice (Figure 2c and e). Taken together, whereas initially higher levels of energy equivalents are produced upon Ketamine injection, they are reduced again at 24 h and return to normal levels at the 72-h time point.

Results from previous studies have associated the antidepressant treatment response with drugs elevating ATP levels. Phosphorous-31 magnetic resonance spectroscopy data have shown decreased NPT levels (mainly ATP) in the brain of depressed patients. Another magnetic resonance spectroscopy study could demonstrate lower NPT levels (mainly ATP) in fluoxetine responders compared with nonresponders.[62,63] These

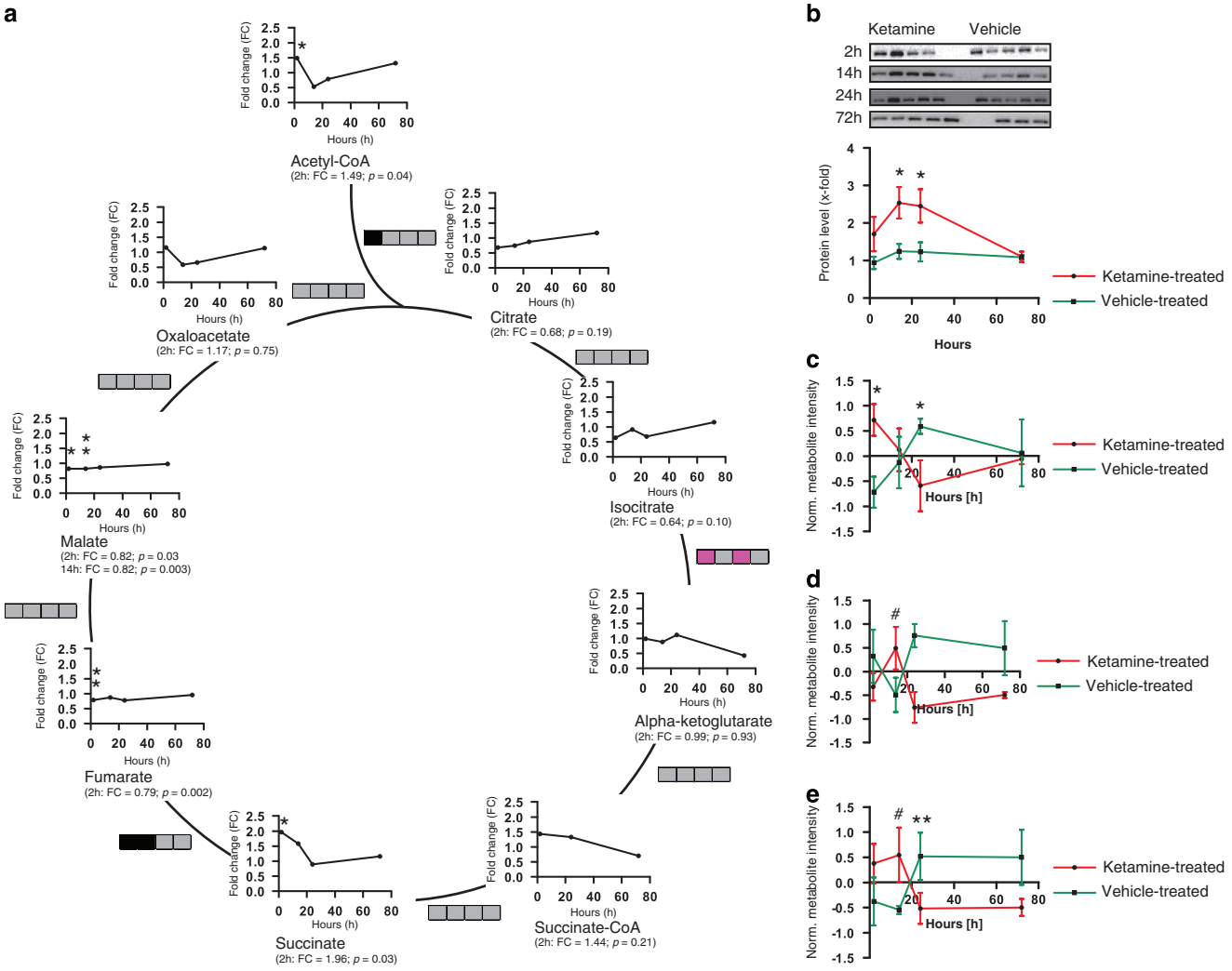

Figure 2. Citrate cycle metabolite level, metabolite ratio and energy status analyses upon Ketamine treatment (3 mg kg $^{-1}$) of 2-, 14-, 24- and 72-h time points. (**a**) Citrate cycle time course showing metabolite fold change (FC) and metabolite ratios. Metabolite ratios are indicated by boxes and each box represents a time point (from left to right 2, 14, 24 and 72 h). Significant metabolite ratio differences or trends are illustrated in pink (increased ratio) and black (decreased ratio). $N = 5$ mice per group and time point. (**b**) Western blot analysis of succinate dehydrogenase complex, subunit A (SDHA) from Ketamine- and vehicle-treated mice hippocampi, 2 h (1.705 ± 0.4583, Ketamine-treated, $n = 4$; 0.9417 ± 0.1633, vehicle-treated, $n = 5$), $P = 0.1285$, 14 h (2.539 ± 0.4195, Ketamine-treated, $n = 5$; 1.247 ± 0.1988, vehicle-treated, $n = 4$), $P = 0.0381$, 24 h (2.456 ± 0.4456, Ketamine-treated, $n = 5$; 1.234 ± 0.2532, vehicle-treated, $n = 5$) and 72 h (1.103 ± 0.1382, Ketamine-treated, $n = 5$; 1.085 ± 0.06048, vehicle-treated, $n = 3$) after treatment. Energy-state analyses of (**c**) GTP, (**d**) NADH and (**e**) ATP 2, 14, 24 and 72 h after Ketamine treatment ($n = 5$). $^{\#}P \leqslant 0.10$, $^{*}P \leqslant 0.05$, $^{**}P \leqslant 0.01$. *P*-values were determined by Student's *t*-test. Error bars represent s.e.m.

inconsistent findings make it difficult to know whether our observations of initially increased or later decreased ATP levels contribute to the antidepressant-like effect for Ketamine. Previous data from a study in rats have suggested that the antidepressant-like effect observed after a single injection of Ketamine is mediated by an increased anabolic rate-mediating cell growth and differentiation. An elevated anabolism might be mediated through a higher energy demand, which we indeed observed 2 and 14 h after Ketamine treatment. The glycolytic pathway was also found to be enriched upon Ketamine treatment (Table 1). Almost all metabolites of this pathway show lower levels (glucose-6-phosphate, fructose-6-phosphate, fructose-1,6-bisphosphate, dihydroxy-acetone-phosphate and glyceraldehyde-3-phosphate) 14 h after Ketamine injection, with the exception of 3-phosphoglycerate and phosphoenolpyruvate that are upregulated at the 2-h time point. The observed changes might be caused by a feedback mechanism of the citrate cycle, which can have an impact on glycolysis by either activating or inhibiting it or by the metabolite ratio changes (fructose-6-phosphate/glucose-6-phosphate, fructose-1,6-phospate/fructose-6-phosphate, glyceraldehyde-3-phosphate/dihydroxy-acetone-phosphate, 3-phosphoglycerate/glyceraldehyde-3-phosphate, 3-phosphoglycerate/phosphoenolpyruvate and pyruvate/phosphoenolpyruvate) of the glycolysis pathway indicating altered enzyme activities or protein expression. Interestingly, whereas we found a reduced glycolysis pathway activity after Ketamine treatment, a previous study has shown an elevation of glycolytic metabolites following SSRI treatment, suggesting that the two drug types have very different modes of action.[47] The rapid increase in newly synthesized synaptic proteins and spines upon Ketamine treatment is known to be initiated through the activation of mammalian target of rapamycin. Neither conventional antidepressants such as imipramine and fluoxetine acutely or chronically administered nor electroconvulsive shock activate mammalian target of rapamycin.[23] Moreover, it was observed that the SSRI sertraline inhibits mammalian target of rapamycin.[64] All these

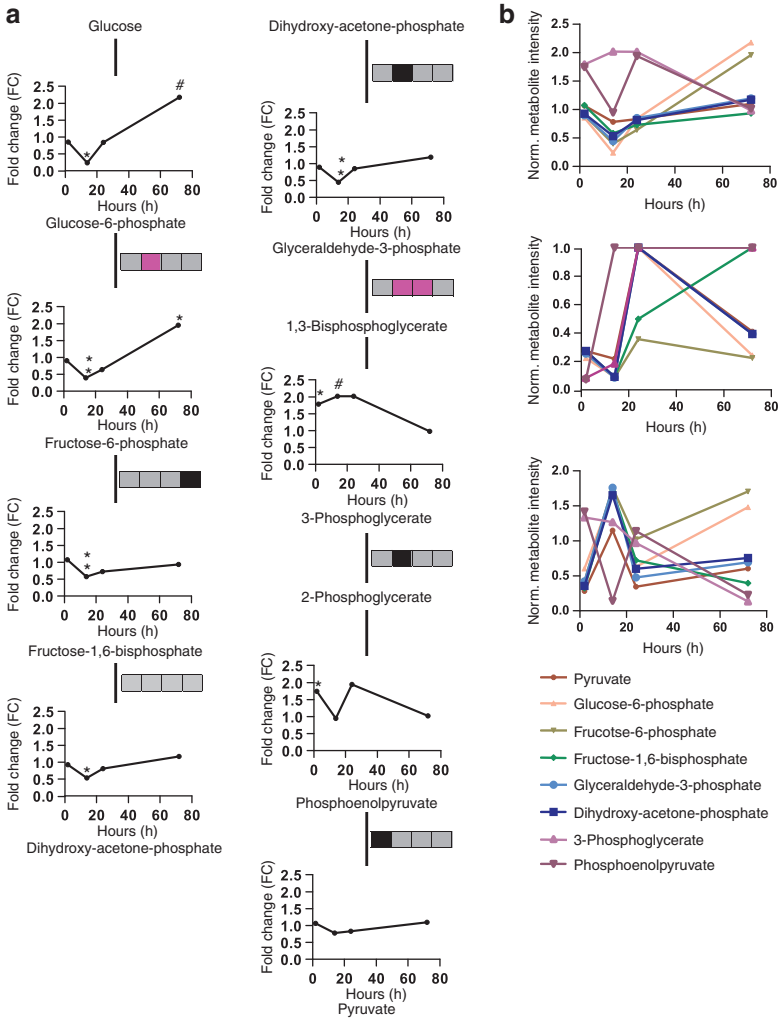

Figure 3. Glycolytic metabolite levels and metabolite ratios and fold change (FC), variable influence of projection (VIP) score and *q*-value comparisons of all quantified glycolytic metabolites at 2-, 14-, 24- and 72-h time points after Ketamine treatment (3 mg kg^{-1}). (**a**) Glycolysis/gluconeogenesis time course metabolite FCs and ratios. Metabolite ratios are indicated by boxes and each box represents a time point (from left to right 2, 14, 24 and 72 h). Significant metabolite ratio differences or trends are illustrated in pink (increased ratio) and black (decreased ratio). (**b**) Comparison of the FCs, *q*-values and VIP scores of all metabolites of the glycolytic pathway. $N = 5$ mice per group and time point. $^{\#}P \leqslant 0.10$, $^{*}P \leqslant 0.05$, $^{**}P \leqslant 0.01$. *P*-values were determined by Student's *t*-test.

findings might explain the delayed onset of conventional antidepressants and the opposite findings with regard to pathway activity between conventional SSRI antidepressants and Ketamine.

Whereas acute treatment of rodents with Ketamine at low levels reduces depressive-like behavior as assessed by the FST immobility time, higher doses of the drug chronically administered for 10 days have the opposite effect using the same behavioral assay.[65] Already at smaller doses (6 mg kg^{-1}) Ketamine also induces prepulse inhibition deficits, known to be impaired in schizophrenia, that can be reversed by antipsychotics.[66,67] Furthermore, chronically injected high subanesthetic doses of Ketamine produce positive, negative and cognitive schizophrenia-like symptoms in healthy humans[68] and rodents.[65] For all these reasons, Ketamine treatment is also used to generate animal models of schizophrenia.

A possible explanation for the different acute and chronic Ketamine treatment effects might be the involvement of different receptor types. Acute Ketamine treatment has been reported to only block NMDAR on GABAergic neurons, whereas chronic treatment with high doses not only blocks NMDARs universally but also nicotinic acetylcholine receptors.[69]

Alterations in metabolite, transcript and protein levels in *post-mortem* tissue from schizophrenic patients have been reported for glycolysis, citrate cycle and OXPHOS, the same pathways observed to be affected in the present study.[70–72] As Ketamine at higher doses can induce schizophrenia-like symptoms, it is conceivable that certain molecular pathways are shared between the antidepressant and psychotic effects. At the same time there must be differences in other affected pathways responsible for the opposite effects of the drug. Owing to its psychomimetic side effects Ketamine is not used as a first-line drug to treat MDD in the clinic. An improved understanding of the molecular events causing the antidepressant effect of Ketamine will help in developing alternative fast-acting drugs with a similar mode of action.

Finally, we were also interested in exploiting our metabolomics analysis data to identify a biosignature for the Ketamine drug response. PLS-DA and VIP score analyses revealed that 2-ketoisovalerate, glutathione, maleate, methylmalonate, SBP, fumarate and cytosine represent stable and consistent metabolite biomarkers for all time points (Supplementary Figure 2B).

We only assessed Ketamine's behavioral effect using FST immobility time. We did not carry out any additional behavioral analyses including Learned Helplessness, Chronic Mild Stress and Novelty Suppressed Feeding Test that have been reported by others.[17–22] Performing several consecutive behavioral assays might affect the animals' metabolome and skew the data. Other limitations of our study include the limited number of animals that were used for the metabolomic analyses ($n = 5$) and the relatively large number of metabolites quantified (> 200), which could result in false discoveries.

Future metabolomic analyses of other brain regions relevant for MDD including the prefrontal cortex, thalamus and amygdala will further our understanding of Ketamine's mode of action and the antidepressant effect. Repeating our studies with an animal model of depression will add further relevance to the human situation.

CONFLICT OF INTEREST

The authors declare no conflict of interest.

ACKNOWLEDGMENTS

This work was supported by the *Max Planck Society*. KW was supported by the International Max Planck Research School for Molecular and Cellular Life Sciences (IMPRS-LS).

REFERENCES

1 Kessler RC, Berglund P, Demler O, Jin R, Koretz D, Merikangas KR *et al.* The epidemiology of major depressive disorder: results from the National Comorbidity Survey Replication (NCS-R). *JAMA* 2003; **289**: 3095–3105.
2 Hashimoto K. The role of glutamate on the action of antidepressants. *Prog Neuropsychopharmacol Biol Psychiatry* 2011; **35**: 1558–1568.
3 Trivedi MH, Rush AJ, Wisniewski SR, Nierenberg AA, Warden D, Ritz L *et al.* Evaluation of outcomes with citalopram for depression using measurement-based care in STAR*D: implications for clinical practice. *Am J Psychiatry* 2006; **163**: 28–40.
4 Hirota K, Lambert DG. Ketamine: its mechanism(s) of action and unusual clinical uses. *Br J Anaesth* 1996; **77**: 441–444.
5 Berman RM, Cappiello A, Anand A, Oren DA, Heninger GR, Charney DS *et al.* Antidepressant effects of ketamine in depressed patients. *Biol Psychiatry* 2000; **47**: 351–354.
6 Krystal JH, D'Souza DC, Petrakis IL, Belger A, Berman RM, Charney DS *et al.* NMDA agonists and antagonists as probes of glutamatergic dysfunction and pharmacotherapies in neuropsychiatric disorders. *Harv Rev Psychiatry* 1999; **7**: 125–143.
7 Javitt DC. Glutamate as a therapeutic target in psychiatric disorders. *Mol Psychiatry* 2004; **9**: 984–997, 979.
8 aan het Rot M, Collins KA, Murrough JW, Perez AM, Reich DL, Charney DS *et al.* Safety and efficacy of repeated-dose intravenous ketamine for treatment-resistant depression. *Biol Psychiatry* 2010; **67**: 139–145.
9 Diazgranados N, Ibrahim L, Brutsche NE, Newberg A, Kronstein P, Khalife S *et al.* A randomized add-on trial of an N-methyl-D-aspartate antagonist in treatment-resistant bipolar depression. *Arch Gen Psychiatry* 2010; **67**: 793–802.
10 DiazGranados N, Ibrahim LA, Brutsche NE, Ameli R, Henter ID, Luckenbaugh DA *et al.* Rapid resolution of suicidal ideation after a single infusion of an N-methyl-D-aspartate antagonist in patients with treatment-resistant major depressive disorder. *J Clin Psychiatry* 2010; **71**: 1605–1611.
11 Larkin GL, Beautrais AL. A preliminary naturalistic study of low-dose ketamine for depression and suicide ideation in the emergency department. *Int J Neuropsychopharmacol* 2011; **14**: 1127–1131.
12 Machado-Vieira R, Salvadore G, Diazgranados N, Zarate CA. Ketamine and the next generation of antidepressants with a rapid onset of action. *Pharmacol Ther* 2009; **123**: 143–150.
13 Mathew SJ, Murrough JW, aan het Rot M, Collins KA, Reich DL, Charney DS. Riluzole for relapse prevention following intravenous ketamine in treatment-resistant depression: a pilot randomized, placebo-controlled continuation trial. *Int J Neuropsychopharmacol* 2010; **13**: 71–82.
14 Phelps LE, Brutsche N, Moral JR, Luckenbaugh DA, Manji HK, Zarate CA. Family history of alcohol dependence and initial antidepressant response to an N-methyl-D-aspartate antagonist. *Biol Psychiatry* 2009; **65**: 181–184.
15 Price RB, Nock MK, Charney DS, Mathew SJ. Effects of intravenous ketamine on explicit and implicit measures of suicidality in treatment-resistant depression. *Biol Psychiatry* 2009; **66**: 522–526.
16 Zarate CA, Singh JB, Carlson PJ, Brutsche NE, Ameli R, Luckenbaugh DA *et al.* A randomized trial of an N-methyl-D-aspartate antagonist in treatment-resistant major depression. *Arch Gen Psychiatry* 2006; **63**: 856–864.
17 Autry AE, Adachi M, Nosyreva E, Na ES, Los MF, Cheng PF *et al.* NMDA receptor blockade at rest triggers rapid behavioural antidepressant responses. *Nature* 2011; **475**: 91–95.
18 Garcia LS, Comim CM, Valvassori SS, Réus GZ, Barbosa LM, Andreazza AC *et al.* Acute administration of ketamine induces antidepressant-like effects in the forced swimming test and increases BDNF levels in the rat hippocampus. *Prog Neuropsychopharmacol Biol Psychiatry* 2008; **32**: 140–144.
19 Garcia LS, Comim CM, Valvassori SS, Réus GZ, Stertz L, Kapczinski F *et al.* Ketamine treatment reverses behavioral and physiological alterations induced by chronic mild stress in rats. *Prog Neuropsychopharmacol Biol Psychiatry* 2009; **33**: 450–455.
20 Koike H, Iijima M, Chaki S. Involvement of AMPA receptor in both the rapid and sustained antidepressant-like effects of ketamine in animal models of depression. *Behav Brain Res* 2011; **224**: 107–111.
21 Li N, Liu RJ, Dwyer JM, Banasr M, Lee B, Son H *et al.* Glutamate N-methyl-D-aspartate receptor antagonists rapidly reverse behavioral and synaptic deficits caused by chronic stress exposure. *Biol Psychiatry* 2011; **69**: 754–761.
22 Maeng S, Zarate CA, Du J, Schloesser RJ, McCammon J, Chen G *et al.* Cellular mechanisms underlying the antidepressant effects of ketamine: role of alpha-amino-3-hydroxy-5-methylisoxazole-4-propionic acid receptors. *Biol Psychiatry* 2008; **63**: 349–352.
23 Li N, Lee B, Liu RJ, Banasr M, Dwyer JM, Iwata M *et al.* mTOR-dependent synapse formation underlies the rapid antidepressant effects of NMDA antagonists. *Science* 2010; **329**: 959–964.
24 Kessler RC. The effects of stressful life events on depression. *Annu Rev Psychol* 1997; **48**: 191–214.
25 Thomas RM, Hotsenpiller G, Peterson DA. Acute psychosocial stress reduces cell survival in adult hippocampal neurogenesis without altering proliferation. *J Neurosci* 2007; **27**: 2734–2743.
26 Malberg JE, Duman RS. Cell proliferation in adult hippocampus is decreased by inescapable stress: reversal by fluoxetine treatment. *Neuropsychopharmacology* 2003; **28**: 1562–1571.
27 Pham K, Nacher J, Hof PR, McEwen BS. Repeated restraint stress suppresses neurogenesis and induces biphasic PSA-NCAM expression in the adult rat dentate gyrus. *Eur J Neurosci* 2003; **17**: 879–886.
28 Vermetten E, Bremner JD. Circuits and systems in stress. II. Applications to neurobiology and treatment in posttraumatic stress disorder. *Depress Anxiety* 2002; **16**: 14–38.
29 Koolschijn PC, van Haren NE, Lensvelt-Mulders GJ, Hulshoff Pol HE, Kahn RS. Brain volume abnormalities in major depressive disorder: a meta-analysis of magnetic resonance imaging studies. *Hum Brain Mapp* 2009; **30**: 3719–3735.
30 Kempton MJ, Salvador Z, Munafò MR, Geddes JR, Simmons A, Frangou S *et al.* Structural neuroimaging studies in major depressive disorder. Meta-analysis and comparison with bipolar disorder. *Arch Gen Psychiatry* 2011; **68**: 675–690.
31 Arnone D, McIntosh AM, Ebmeier KP, Munafò MR, Anderson IM. Magnetic resonance imaging studies in unipolar depression: systematic review and meta-regression analyses. *Eur Neuropsychopharmacol* 2012; **22**: 1–16.
32 Arnone D, McKie S, Elliott R, Juhasz G, Thomas EJ, Downey D *et al.* State-dependent changes in hippocampal grey matter in depression. *Mol Psychiatry* 2013; **18**: 1265–1272.
33 McEwen BS, Magarinos AM. Stress and hippocampal plasticity: implications for the pathophysiology of affective disorders. *Hum Psychopharmacol* 2001; **16**: S7–S19.
34 Reagan LP, McEwen BS. Controversies surrounding glucocorticoid-mediated cell death in the hippocampus. *J Chem Neuroanat* 1997; **13**: 149–167.
35 Cameron HA, Tanapat P, Gould E. Adrenal steroids and N-methyl-D-aspartate receptor activation regulate neurogenesis in the dentate gyrus of adult rats through a common pathway. *Neuroscience* 1998; **82**: 349–354.
36 Rajkowska G. Postmortem studies in mood disorders indicate altered numbers of neurons and glial cells. *Biol Psychiatry* 2000; **48**: 766–777.
37 Zakzanis KK, Leach L, Kaplan E. On the nature and pattern of neurocognitive function in major depressive disorder. *Neuropsychiatry Neuropsychol Behav Neurol* 1998; **11**: 111–119.
38 Frodl T, Bokde AL, Scheuerecker J, Lisiecka D, Schoepf V, Hampel H *et al.* Functional connectivity bias of the orbitofrontal cortex in drug-free patients with major depression. *Biol Psychiatry* 2010; **67**: 161–167.
39 Kaddurah-Daouk R, Krishnan KR. Metabolomics: a global biochemical approach to the study of central nervous system diseases. *Neuropsychopharmacology* 2009; **34**: 173–186.
40 Fiehn O. Metabolomics--the link between genotypes and phenotypes. *Plant Mol Biol* 2002; **48**: 155–171.
41 Filiou MD, Turck CW, Martins-de-Souza D. Quantitative proteomics for investigating psychiatric disorders. *Proteomics Clin Appl* 2011; **5**: 38–49.

42 Tusher VG, Tibshirani R, Chu G. Significance analysis of microarrays applied to the ionizing radiation response. *Proc Natl Acad Sci USA* 2001; **98**: 5116–5121.
43 Xia J, Psychogios N, Young N, Wishart DS. MetaboAnalyst: a web server for metabolomic data analysis and interpretation. *Nucleic Acids Res* 2009; **37**: W652–W660.
44 Svante W, Michael S, Lennart E. PLS-regression: a basic tool of chemometrics. *Chemometr Intell Lab Syst* 2001; **58**: 109–130.
45 Hosack DA, Dennis G, Sherman BT, Lane HC, Lempicki RA. Identifying biological themes within lists of genes with EASE. *Genome Biol* 2003; **4**: R70.
46 Freeman LC. A set of measures of centrality based upon betweenness. *Sociometry* 1977; **40**: 35–41.
47 Webhofer C, Gormanns P, Reckow S, Lebar M, Maccarrone G, Ludwig T *et al.* Proteomic and metabolomic profiling reveals time-dependent changes in hippocampal metabolism upon paroxetine treatment and biomarker candidates. *J Psychiatr Res* 2013; **47**: 289–298.
48 Filiou MD, Zhang Y, Teplytska L, Reckow S, Gormanns P, Maccarrone G *et al.* Proteomics and metabolomics analysis of a trait anxiety mouse model reveals divergent mitochondrial pathways. *Biol Psychiatry* 2011; **70**: 1074–1082.
49 Scaini G, Santos PM, Benedet J, Rochi N, Gomes LM, Borges LS *et al.* Evaluation of Krebs cycle enzymes in the brain of rats after chronic administration of antidepressants. *Brain Res Bull* 2010; **82**: 224–227.
50 Petersen AK, Krumsiek J, Wägele B, Theis FJ, Wichmann HE, Gieger C *et al.* On the hypothesis-free testing of metabolite ratios in genome-wide and metabolome-wide association studies. *BMC Bioinformatics* 2012; **13**: 120.
51 Su ZH, Li SQ, Zou GA, Yu CY, Sun YG, Zhang HW *et al.* Urinary metabonomics study of anti-depressive effect of Chaihu-Shu-Gan-San on an experimental model of depression induced by chronic variable stress in rats. *J Pharm Biomed Anal* 2011; **55**: 533–539.
52 Dai Y, Li Z, Xue L, Dou C, Zhou Y, Zhang L *et al.* Metabolomics study on the antidepression effect of xiaoyaosan on rat model of chronic unpredictable mild stress. *J Ethnopharmacol* 2010; **128**: 482–489.
53 Ji Y, Hebbring S, Zhu H, Jenkins GD, Biernacka J, Snyder K *et al.* Glycine and a glycine dehydrogenase (GLDC) SNP as citalopram/escitalopram response biomarkers in depression: pharmacometabolomics-informed pharmacogenomics. *Clin Pharmacol Ther* 2011; **89**: 97–104.
54 Watkins SM, German JB. Metabolomics and biochemical profiling in drug discovery and development. *Curr Opin Mol Ther* 2002; **4**: 224–228.
55 Scaini G, Maggi DD, De-Nês BT, Gonçalves CL, Ferreira GK, Teodorak BP *et al.* Activity of mitochondrial respiratory chain is increased by chronic administration of antidepressants. *Acta Neuropsychiatr* 2011; **23**: 112–118.
56 Rollins B, Martin MV, Sequeira PA, Moon EA, Morgan LZ, Watson SJ *et al.* Mitochondrial variants in schizophrenia, bipolar disorder, and major depressive disorder. *PLoS ONE* 2009; **4**: e4913.
57 Kazuno AA, Munakata K, Mori K, Nanko S, Kunugi H, Nakamura K *et al.* Mitochondrial DNA haplogroup analysis in patients with bipolar disorder. *Am J Med Genet B Neuropsychiatr Genet* 2009; **150B**: 243–247.
58 Kato T, Kunugi H, Nanko S, Kato N. Association of bipolar disorder with the 5178 polymorphism in mitochondrial DNA. *Am J Med Genet* 2000; **96**: 182–186.
59 Kato T, Kato N. Mitochondrial dysfunction in bipolar disorder. *Bipolar Disord* 2000; **2**: 180–190.
60 Murashita J, Kato T, Shioiri T, Inubushi T, Kato N. Altered brain energy metabolism in lithium-resistant bipolar disorder detected by photic stimulated 31P-MR spectroscopy. *Psychol Med* 2000; **30**: 107–115.
61 Glancy B, Balaban RS. Role of mitochondrial Ca2+ in the regulation of cellular energetics. *Biochemistry* 2012; **51**: 2959–2973.
62 Moore CM, Christensen JD, Lafer B, Fava M, Renshaw PF. Lower levels of nucleoside triphosphate in the basal ganglia of depressed subjects: a phosphorous-31 magnetic resonance spectroscopy study. *Am J Psychiatry* 1997; **154**: 116–118.
63 Volz HP, Rzanny R, Riehemann S, May S, Hegewald H, Preussler B *et al.* 31P magnetic resonance spectroscopy in the frontal lobe of major depressed patients. *Eur Arch Psychiatry Clin Neurosci* 1998; **248**: 289–295.
64 Lin CJ, Robert F, Sukarieh R, Michnick S, Pelletier J. The antidepressant sertraline inhibits translation initiation by curtailing mammalian target of rapamycin signaling. *Cancer Res* 2010; **70**: 3199–3208.
65 Chatterjee M, Ganguly S, Srivastava M, Palit G. Effect of 'chronic' versus 'acute' ketamine administration and its 'withdrawal' effect on behavioural alterations in mice: implications for experimental psychosis. *Behav Brain Res* 2011; **216**: 247–254.
66 Swerdlow NR, Taaid N, Oostwegel JL, Randolph E, Geyer MA. Towards a cross-species pharmacology of sensorimotor gating: effects of amantadine, bromocriptine, pergolide and ropinirole on prepulse inhibition of acoustic startle in rats. *Behav Pharmacol* 1998; **9**: 389–396.
67 Cilia J, Hatcher P, Reavill C, Jones DN. (+/−) Ketamine-induced prepulse inhibition deficits of an acoustic startle response in rats are not reversed by antipsychotics. *J Psychopharmacol* 2007; **21**: 302–311.
68 Javitt DC, Zukin SR. Recent advances in the phencyclidine model of schizophrenia. *Am J Psychiatry* 1991; **148**: 1301–1308.
69 Chatterjee M, Verma R, Ganguly S, Palit G. Neurochemical and molecular characterization of ketamine-induced experimental psychosis model in mice. *Neuropharmacology* 2012; **63**: 1161–1171.
70 Martins-de-Souza D, Gattaz WF, Schmitt A, Rewerts C, Maccarrone G, Dias-Neto E *et al.* Prefrontal cortex shotgun proteome analysis reveals altered calcium homeostasis and immune system imbalance in schizophrenia. *Eur Arch Psychiatry Clin Neurosci* 2009; **259**: 151–163.
71 Prabakaran S, Swatton JE, Ryan MM, Huffaker SJ, Huang JT, Griffin JL *et al.* Mitochondrial dysfunction in schizophrenia: evidence for compromised brain metabolism and oxidative stress. *Mol Psychiatry* 2004; **9**: 684–697, 643.
72 Altar CA, Jurata LW, Charles V, Lemire A, Liu P, Bukhman Y *et al.* Deficient hippocampal neuron expression of proteasome, ubiquitin, and mitochondrial genes in multiple schizophrenia cohorts. *Biol Psychiatry* 2005; **58**: 85–96.

Supplementary Information accompanies the paper on the Translational Psychiatry website (http://www.nature.com/tp)